(2)

IDA MEMORANDUM REPORT M-548

CENTRAL RESEARCH PROJECT REPORT ON SUPERCONDUCTIVITY (1988): PART I, MATERIALS AND IR DETECTORS

William S. Hong
John E. Hove
Mark S. Taylor

December 1988

INSTITUTE FOR DEFENSE ANALYSES
1801 N. Beauregard Street, Alexandria, Virginia 22311

IDA Log No. HQ 88-34698

DEFINITIONS

IDA publishes the following documents to report the results of its work.

Reports

Reports are the most authoritative and most carefully considered products IDA publishes. They normally embody results of major projects which (a) have a direct bearing on decisions affecting major programs, or (b) address issues of significant concern to the Executive Branch, the Congress and/or the public, or (c) address issues that have significant economic implications. IDA Reports are reviewed by outside panels of experts to ensure their high quality and relevance to the problems studied, and they are released by the President of IDA.

Papers

Papers normally address relatively restricted technical or policy issues. They communicate the results of special analyses, interim reports or phases of a task, ad hoc or quick reaction work. Papers are reviewed to ensure that they meet standards similar to those expected of refereed papers in professional journals.

Memorandum Reports

IDA Memorandum Reports are used for the convenience of the sponsors or the analysts to record substantive work done in quick reaction studies and major interactive technical support activities; to make available preliminary and tentative results of analyses or of working group and panel activities; to forward information that is essentially unanalyzed and unevaluated; or to make a record of conferences, meetings, or briefings, or of data developed in the course of an investigation. Review of Memorandum Reports is suited to their content and intended use.

The results of IDA work are also conveyed by briefings and informal memoranda to sponsors and others designated by the sponsors, when appropriate.

The work reported in this document was conducted under IDA's Independent Research Program. Its publication does not imply endorsement by the Department of Defense or any other government agency, nor should the contents be construed as reflecting the official position of any government agency.

REPORT DOCUMENTATION PAGE

1a. REPORT SECURITY CLASSIFICATION UNCLASSIFIED	1b. RESTRICTIVE MARKINGS
2a. SECURITY CLASSIFICATION AUTHORITY N/A	3. DISTRIBUTION/AVAILABILITY OF REPORT This document is unclassified and suitable for public release.
2b. DECLASSIFICATION/DOWNGRADING SCHEDULE N/A	
4. PERFORMING ORGANIZATION REPORT NUMBER(S) IDA Memorandum Report M-548	5. MONITORING ORGANIZATION REPORT NUMBER(S)
6a. NAME OF PERFORMING ORGANIZATION Institute for Defense Analyses 6b. OFFICE SYMBOL (If applicable)	7a. NAME OF MONITORING ORGANIZATION
6c. ADDRESS (City, State, and Zip Code) 1801 N. Beauregard Street Alexandria, VA 22311-1772	7b. ADDRESS (CITY, STATE, AND ZIP CODE)
8a. NAME OF FUNDING/SPONSORING ORGANIZATION 8b. OFFICE SYMBOL (If applicable)	9. PROCUREMENT INSTRUMENT IDENTIFICATION NUMBER IDA Independent Research Program
8c. ADDRESS (City, State, and Zip Code)	10. SOURCE OF FUNDING NUMBERS PROGRAM ELEMENT: PROJECT NO.: TASK NO.: CRP WORK UNIT ACCESSION NO.:

11. TITLE (Include Security Classification)
Central Research Project Report on Superconductivity (1988): Part I, Materials and IR Detectors

12. PERSONAL AUTHOR(S).
William S. Hong, John E. Hove, Mark S. Taylor

13. TYPE OF REPORT	13b. TIME COVERED	14. DATE OF REPORT (Year, Month, Day)	15. PAGE COUNT
Final	FROM 3/88 TO 9/88	December 1988	37

16. SUPPLEMENTARY NOTATION

17. COSATI CODES			18. SUBJECT TERMS (Continue on reverse if necessary and identify by block number)
FIELD	GROUP	SUB-GROUP	Superconductivity, Ceramic superconductors, Infrared detectors, Bolometers, Superconductor IR detectors, Phase Equilibria, Ceramic crystal structures, Superconducting electronic circuits

19. ABSTRACT (Continue on reverse if necessary and identify by block number)

This report reviews and summarizes available information on the phases and crystal structures of known and predicted high-temperature superconductors (HTS). Materials involving thallium have already exhibited critical temperatures up to 125 K, and techniques have been suggested to increase this value. Recent theoretical efforts predict that room-temperature superconducting materials, if possible at all, may require different chemical compositions than those oxides presently under investigation. A second part of the report reviews the possible direct use of HTS as infrared sensor elements. This indicates little or no advantage over semiconductors; however, HTS use in the signal-processing circuitry of detector arrays may be highly beneficial. A second (later) report will describe a quantitative analysis on the feasibility of a self-guided probe weapon using superconducting magnetic field gradient sensors. While additional analysis and calculations are still necessary, the tentative conclusion of this Part II report is that an HTS seeker and guidance system may be feasible for the destruction of tanks, ships, submarines, or other large steel targets. Such a missile would be generally insensitive to the environment or common countermeasures such as flares, camouflage, or smoke screens.

20. DISTRIBUTION/AVAILABILITY OF ABSTRACT ☐ UNCLASSIFIED/UNLIMITED ☒ SAME AS RPT. ☐ DTIC USERS	21. ABSTRACT SECURITY CLASSIFICATION UNCLASSIFIED
22a. NAME OF RESPONSIBLE INDIVIDUAL John E. Hove	22b. TELEPHONE (Include Area Code) (703) 578-2869 22c. OFFICE SYMBOL

DD FORM 1473. 84 MAR 83 APR edition may be used until exhausted. All other editions are obsolete

IDA MEMORANDUM REPORT M-548

CENTRAL RESEARCH PROJECT REPORT ON SUPERCONDUCTIVITY (1988): PART I, MATERIALS AND IR DETECTORS

William S. Hong
John E. Hove
Mark S. Taylor

December 1988

IDA

INSTITUTE FOR DEFENSE ANALYSES

IDA Independent Research Program

PREFACE

This Memorandum Report presents partial results of Central Research Project (CRP) studies in the area of high-temperature superconductivity performed during FY 1988. An earlier exploratory study (Ref. 1) provided a brief background on the characteristics of superconductors and some examples of their possible defense applications.

For the FY 1988 CRP effort, two activities are reported herein:

(1) Phase equilibria and crystal structure of known high-temperature superconductors, and

(2) Applications to infrared sensor systems.

In a later report an analysis of gradiometer probe use in missile guidance systems for anti-tank and anti-ship applications will be described.

Some portions of the work were partially supported under two tasks from OSD in FY 1988 (T-D2-509, Army Sensor Applications, and T-D2-566, Superconductivity Issues). The results will be reported to those sponsors with, of course, appropriate credit to the CRP support.

This report has not been subjected to formal review.

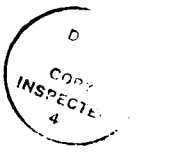

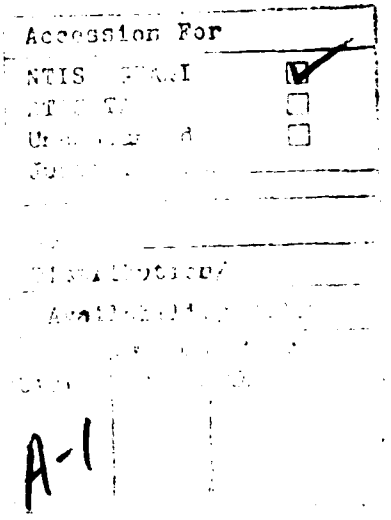

ABSTRACT

This report reviews and summarizes available information on the phases and crystal structures of known and predicted high-temperature superconductors (HTS). Materials involving thallium have already exhibited critical temperatures up to 125 K, and techniques have been suggested to increase this value. Recent theoretical efforts predict that room-temperature superconducting materials, if possible at all, may require different chemical compositions than those oxides presently under investigation. A second part of the report reviews the possible direct use of HTS as infrared sensor elements. This indicates little or no advantage over semiconductors; however, HTS use in the signal-processing circuitry of detector arrays may be highly beneficial. A second (later) report will describe a quantitative analysis on the feasibility of a self-guided probe weapon using superconducting magnetic field gradient sensors. While additional analysis and calculations are still necessary, the tentative conclusion of this Part II report is that an HTS seeker and guidance system may be feasible for the destruction of tanks, ships, submarines, or other large steel targets. Such a missile would be generally insensitive to the environment or common countermeasures such as flares, camouflage, or smoke screens.

CONTENTS

I. INTRODUCTORY REMARKS

In an earlier IDA report (Ref. 1), a general technical background of the superconductivity phenomenon was presented, along with a brief history of the experimental discoveries of increasingly higher critical temperature (T_c) materials since the publication of the initial data on certain mixed oxides in mid-1986 (Ref. 2). Materials of this class have been prepared, to date, with a T_c of 125 K, and there is no reason to believe this value will not continue to increase, nor is there any reason to believe that such oxides are necessarily the only type of compounds to exhibit this behavior. Thus, there is an enormous concentration of research and engineering interest in all technically advanced countries in what has come to be called high-temperature superconductors or HTS (as opposed to conventional low-temperature superconductors, or LTS, which are currently in use at operating temperatures of about 10 K or less). A condensed version of what is known about the phases and crystal structures of the HTS materials is presented in Chapters II and III.

One of the highly publicized near-term applications of superconductivity is improved infrared detector systems, a subject on which IDA has a great deal of expertise. A preliminary analysis is given in Chapters IV and V. An IDA concept for using HTS magnetic field sensors as a detection and guidance system in an anti-tank (or anti-ship) missile showed promise (Ref. 1). Additional computations, to be published in a subsequent report, tend to support this promise.

Known HTS materials are multicomponent oxides (i.e., ceramics) having complicated stability relationships with other compositionally similar, but usually nonsuperconducting, phases. Knowledge of the phase relations, especially involving temperature and oxygen pressure, is essential to gaining insight into optimum processing techniques for these materials. In addition to chemical compositions, the atomic arrangements (or crystal structures) tend to differ from ideal crystallographic forms; this difference (and the understanding of it) will provide the basis for future research intended to create more desirable properties.

As of this writing, four major superconducting oxide systems have been discovered (others are known but their critical temperatures are too low to be of interest).

In chronological order, the first HTS compound is generally acknowledged to be the La-Ba-Cu-O system (T_c about 40 K) discovered by Bednorz and Müller (Ref. 2). The second is the Y-Ba-Cu-O system of which the most studied is $YBa_2Cu_3O_{6+x}$, commonly referred to as the "1-2-3" compound, which can have (depending on the value of "x") a T_c as high as 95 K (Ref. 3). The third and fourth compounds are the Bi-Sr-Ca-Cu-O and Tl-Ba-Ca-Cu-O systems. The latter systems are found to exhibit a T_c as high as 125 K. The phases of these four material systems are discussed in Chapters II and III, which also contain comments about possible future materials.

Considering infrared (IR) detectors, the interest in superconductor detector array elements lies in the thought that such devices might offer an attractive alternative to doped semiconductors for many applications. In particular, space-based systems, when there are cold targets with a low background, may have to operate in a spectral band up to 20 μm or greater. Since this region presents difficulties for the popular mercury-cadmium-telluride detectors, extrinsic silicon is usually considered the semiconductor of choice. Unfortunately, doped Si requires an ambient temperature of around 10 K and thus a relatively heavy and power-consuming cryogenic system is needed. This is undesirable for use on board a satellite. If, on the other hand, HTS detectors could operate in the temperature range of 20 K to 45 K, the system benefits would be large. It is this type of consideration which provides much of the motivation (especially in the Strategic Defense Initiative program) for developing HTS detectors. In the past, work on LTS detectors has focused on two types of devices: bolometers and so-called direct detectors based on Josephson junction tunneling effects. While work on HTS detectors continues to involve the same types of devices, it must be remembered that the HTS materials are relatively new and have many unusual properties. It is therefore possible that entirely different IR detection mechanisms might be developed in the future. This possibility will not be considered in this report, which is concerned with current or near-term devices.

Since a major benefit could accrue to focal plane IR detector arrays (as well as an enormous number of other systems) by the development and use of complex superconducting electronic integrated circuit devices, a short note (Chapter VI) on this subject is included.

II. IDENTIFICATION OF THE HIGH-TEMPERATURE SUPERCONDUCTING PHASES IN THE VARIOUS MULTIPLE OXIDE SYSTEMS

A. La-Ba-Cu-O SYSTEM

Although the trend of research interest to the Y-Ba-Cu-O HTS material after its discovery has led to the relative neglect of the La-Ba-Cu-O and La-Sr-Cu-O oxide systems, it is important to understand the phases of the latter compounds, if only for comparison. Among the limited research known to the authors on the phase relations in either of these systems is a recently published communication (Ref. 4) of the subsolidus (non-liquid) ternary phase diagram for the La_2O_3-BaO-CuO system at 950°C in air (Fig. 1). The numbers refer to ratios between $LaO_{1.5}$, BaO, and CuO.

In the diagram below, the existence of two different HTS compositions can be seen; one is the material originally discovered by Bednorz and Müller (La_{2-x}-Ba_x-Cu-O_4, T_c ~ 36 K), while the other, identified as La_{3-x} Ba_{3+x} $Cu_6O_{14+\delta}$, ($x \approx 1$), is a material with T_c > 90 K and is crystallographically identical to the Y-Ba-Cu-O 1-2-3 material.

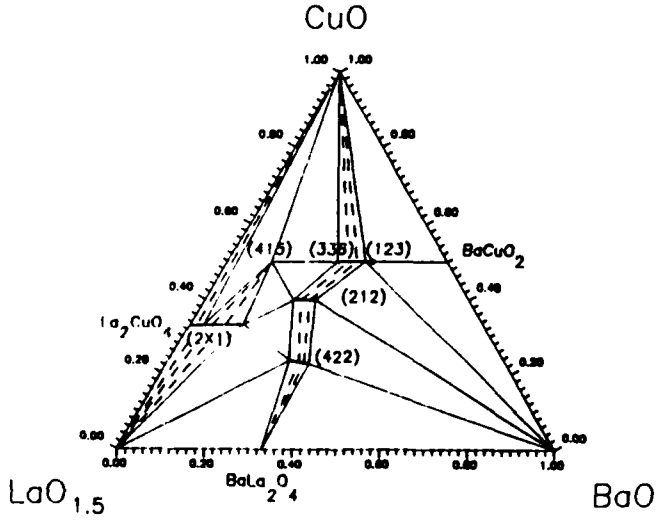

Figure 1. Subsolidus Phase Diagram for the La-Ba-Cu-O System in Air at 950°C. From Ref. 4.

The subsolidus nature of the diagram provides insight into the possible phases that can be encountered during solid state processing of ceramics in this system. Since most of the early fabrication work was accomplished by solid state sintering methods, phase diagrams at isothermal firing temperatures can be used as guides for the mixing of constituent oxides. At this time, apparently, no more comprehensive (non-isothermal) phase diagrams have been published for the La-containing HTS materials.

B. Y-Ba-Cu-O SYSTEM

Several investigators have proposed phase diagrams for this widely studied system; these are, once again, mostly of the ternary isothermal subsolidus type. Even before the phase relationships were systematically determined, however, the superconducting phase in this system was identified as the 1-2-3 compound by Hazen and co-workers (Ref. 5) in collaboration with C.W. Chu of the University of Houston. Hazen also identified a major accompanying phase in Chu's samples as a nonsuperconducting 2-1-1 (Y:Ba:Cu) compound.

Figure 2 is a ternary isothermal phase diagram for the $YO_{1.5}$-BaO-CuO system as determined at 950°C in air by Wang, Mason, et al. at Northwestern University (Ref. 6).

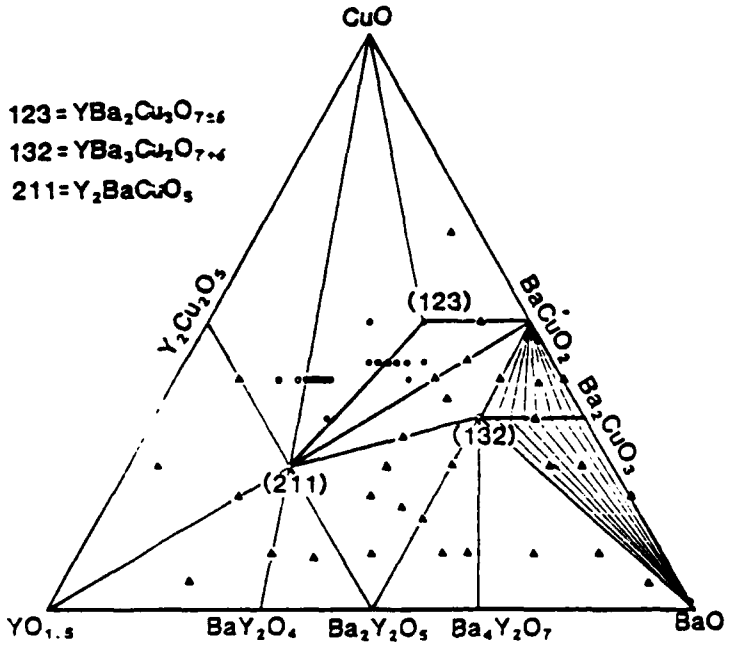

Figure 2. Subsolidus Phase Diagram for the Y-BaO-Cu System in Air at 950°C. From Ref. 6.

Although it differs in some details from the similar diagrams proposed by Frase and Clarke (Ref. 7) and Roth, et al. (Ref. 8), all of these researchers concur that the HTS 1-2-3 material is essentially a "point" compound, compatible with the 2-1-1 material as well as CuO and $BaCuO_2$, but with no appreciable solid solution range. The stability of 1-2-3 compound, its crystal structures, exact composition, and properties are also highly sensitive functions of processing, but these aspects will be discussed later. It should also be noted that the phase equilibria results cited above were preliminary and thought likely to be revised as further research is done.

C. Bi-Sr-Ca-Cu-O AND Tl-Ca-Ba-Cu-O SYSTEMS

To date, several superconducting phases in these newer HTS systems have evidentally been identified, but no detailed phase equilibrium diagrams published. While their higher T_c values (up to 120 K), compared to the superconducting La and Y materials, sparked great attention, a number of structural and chemical characteristics make these newer HTS oxides distinct from the earlier ceramics. Among these are the crystal structure and the lack of rare earth elements in the Bi and Tl systems. The crystallographic differences also contribute to a different crystal morphology in the higher T_c materials; for example, the bismuth compound exhibits platey, highly anisotropic habits with cleavage behavior that makes it appear especially mica-like (Ref. 9).

Another feature that separates these newly discovered HTS oxides from the older materials is that these systems define classes of HTS phases, rather than just one or two compositions. At least one HTS phase has been identified in the Bi-containing system (a second one is thought to exist as a modification of the first) (Ref. 10), while three have been identified so far in the thallium-containing materials, including a "precursor" material lacking calcium (Ref. 9).

Work on the bismuth compounds began in earnest after the discovery by Michel, et al. (Ref. 11) of 22 K T_c superconductivity in the Bi-Sr-Cu-O system.* Later, both Maeda with co-workers in Japan and Chu's group independently induced HTS behavior in the Bi system by adding Ca, and Ca and Al, respectively (Refs. 9 and 12). Later work in the Ca-only containing material identified one of the HTS phases as approximately

---

* Despite the relatively low T_c, this material excited interest because it does not contain a rare earth element, the first such material discovered in the present class of high-temperature superconductors.

$Bi_2CaSr_2Cu_2O_9$ (T_c ~ 90 K) (Ref. 10). Other material fabricated in Chu's group show even higher T_c values near 115 K (Ref. 12).

The first of the thallium materials was announced at nearly the same time, an 81 K T_c Tl-Ba-Cu-O ceramic discovered by Sheng and Hermann. The stoichiometry of the superconducting phase has apparently been determined to be approximately Tl_2 Ba_2 Cu O_{6+x} (Ref. 13). Sheng and Hermann later added calcium to their material and observed an increase in T_c to about 105 K, while independent work by Grant and co-workers at IBM-Almaden confirmed that one of the other phases isolated by Hazen et al. became superconductive at about 125 K, the highest T_c HTS material discovered to date (Ref. 14). All three materials are structurally similar to each other (and to the Bi-containing HTS compounds), with the 105 K superconductor identified as $Tl_2CaBa_2Cu_2O_{8+x}$ and the 125 K HTS oxide as $Tl_2Ca_2Ba_2Cu_3O_{10+x}$. More discussion of how these materials are structurally related to each other will be given in the next section.

III. CRYSTAL STRUCTURES OF THE HIGH-TEMPERATURE SUPERCONDUCTING OXIDE SYSTEMS

A. IDEAL PEROVSKITE CRYSTAL STRUCTURE

The HTS oxides possess, to varying degrees, crystal structures containing blocks that are analogous to the class of materials known as perovskites. An idealized crystal structure is shown by the perovskite unit cell shown in Fig. 3. Perovskites are chemically expressed by the formula ABX_3; a single A cation is located in the center of each unit cell, with eight B cations at each corner and 12 X anions at the middle of all the cube edges. Since each corner B cation is shared by eight other unit cells (when the cell is repeatedly in all three spatial dimensions) and each edge X anion is shared by four other unit cells, the formula ABX_3 is derived.

In a classic perovskite material, the unit cell symmetry is cubic, but lattice distortions that slightly displace ions from their equilibrium positions and change the overall crystal symmetry are common (Barium titanate, $BaTiO_3$, commonly used as a dielectric and piezoelectric material, is a well known perovskite that displays such behavior). The structures of the high T_c superconductors, however, differ from the more conventional perovskites in other significant ways.

B. CRYSTAL STRUCTURES OF THE HTS OXIDES

When describing the crystal structure of even the simplest of the high T_c materials, its complexity requires envisioning stacks of alternating perovskite unit cells such as seen in Fig. 4 for a "perfect" 1-2-3 compound. A cell containing a centrally located Y (or A) ion and Cu (B) ions at the corners is sandwiched between two similar cells with Ba ions located in the central A sites. Oxygen ions are not shown, but would be located at all edge midpoints. Oxygen and copper ions are shared between adjacent cells. It is this stacking of three or more perovskite-like cells that must be used to define a new "unit cell" for the high T_c oxides, which in this particular case, describes a compound with the formula $YBa_2Cu_3O_9$.

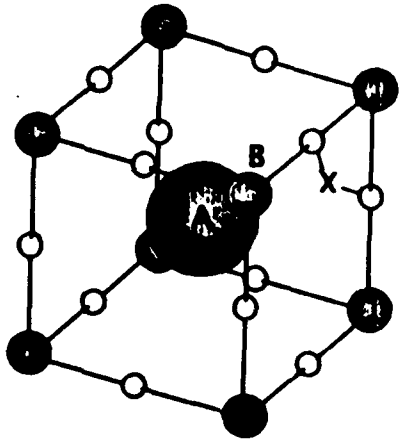

Figure 3. Unit Cell for an Idealized Perovskite ABX_3. Cubic Symmetry is Assumed.

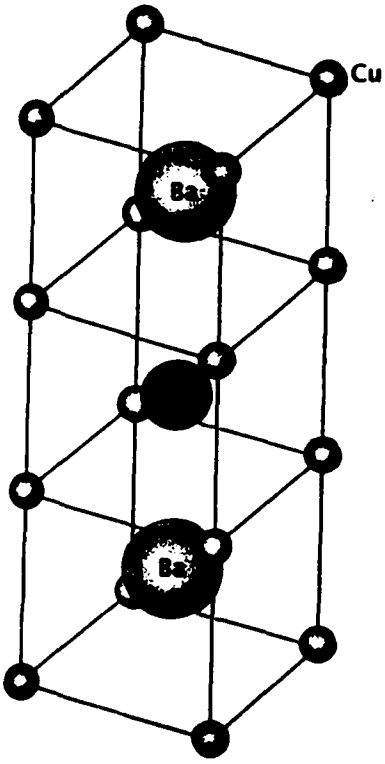

Figure 4. Unit Cell for an Idealized Superconducting Oxide, Formula $YBa_2Cu_3O_9$. (Oxygen ions are not shown, but would normally reside on all the edges that make up the three perovskite-like subcells, midway between the Cu ions). From Ref. 5.

Since the actual HTS oxide known as the 1-2-3 material was found to have the formula $YBa_2Cu_3O_{7-x}$, it was apparent that defects in the form of missing oxygens were present. The actual oxygen stoichiometry is believed to be dependent on the presence of mixed valency Cu ions, but assuming that the Cu is predominantly in the +2 oxidation state, then the formula for the 1-2-3 oxide is $YBa_2Cu_3O_{6.5}$. Most researchers believe, however, that this formula is an average, representing a mixture of materials with oxygen stoichiometries of both 6 and 7, with the latter being the superior superconductor. Figure 5 (Ref. 15) shows the unit cell for this material as it is presently believed to be. Oxygen ions are missing from all vertical edges of the central yttrium-centered cube and from two of the four basal plane edges at both the top and bottom. Since this triple-decked cube is now considered the "unit cell" for the 1-2-3 material, each of the eight missing oxygens is shared with four other unit cells, thus giving the new stoichiometry of $YBa_2Cu_3O_7$. (For the $YBa_2Cu_3O_6$ cubic cell, the remaining oxygens in the basal planes are also missing.)

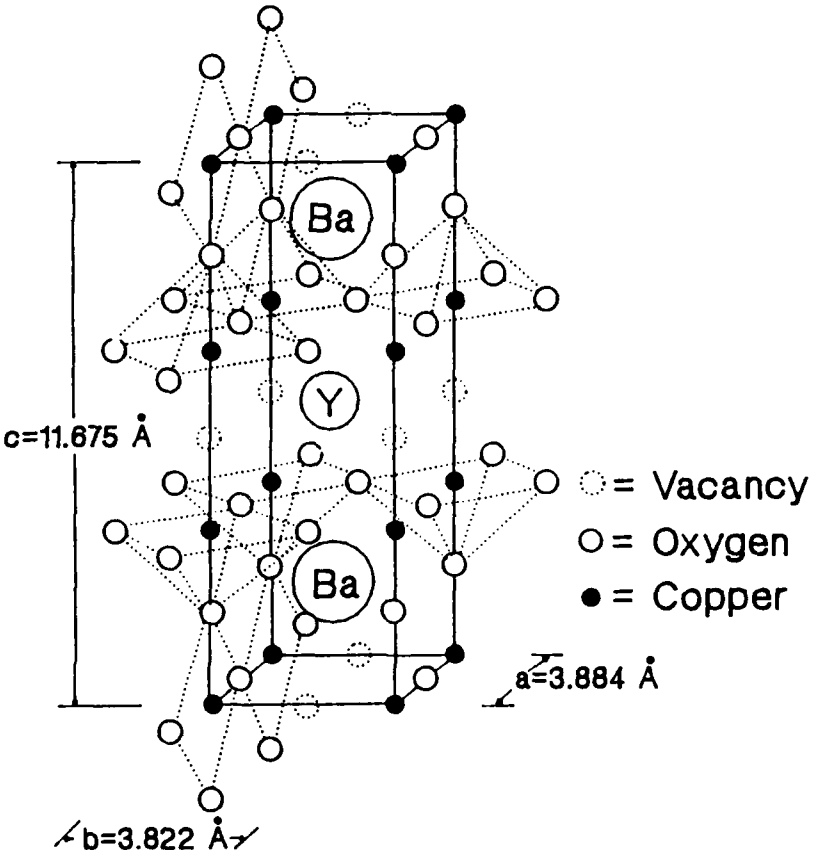

Figure 5. Crystal Structure of the HTS Oxide $YBA_2Cu_3O_7$. The unit cell dimensions of this orthorhombic material are given, while the missing oxygen sites which give its chemical formula are outlined. From Ref. 15.

The crystal symmetry of the 1-2-3 compound is orthorhombic, as can also be seen from Fig. 5 (i.e., the dimensions of the unit cell are unequal, but orthogonal). The structure of the La-Sr-Cu-O superconductor differs slightly, being isostructural with the perovskite known as potassium nickel fluorite, K_2NiF_4 (Ref. 15), which possesses a tetragonal symmetry.

With the advent of the Bi- and Tl-based HTS compounds, the task of describing their crystal structures becomes much more complicated. Although the concept of "stacking" perovskite-based subcells of different chemistries still applies, there are other important differences that take these new materials further away from the simple perovskite unit cell. A sense of this increased complexity can be seen in Fig. 6, which illustrates the atomic arrangements in the the three thallium-based HTS compounds discovered to date, along with a conjectured fourth compound with an even higher T_c (the bismuth materials discovered so far have analogous stoichiometries, and are thus thought to have identical crystal structures). Once again, these materials have a three-tiered structure; the outer layers contain mostly oxygen and thallium, while the inner regions consist of one or more stackings of perovskite-like subcells.

Figure 6 also illustrates a feature of these newer, more complex HTS oxides that may provide a clue to the superconducting mechanism in these materials, especially with regard to ever higher T_c values: the existence of stacks of two-dimensional copper-oxygen planes. In the 2-0-2-1 (Tl:Ca:Ba:Cu ratio) material containing no calcium, there is only one Cu-O plane, while the 2-1-2-2 and 2-2-2-3 materials have two and three stacked planes, respectively. In each case, the increased number of Cu-O planes occurs with a warmer T_c value, leading to speculation that the presence of more of these planes is a key to raising T_c even further (hence the extrapolation in Fig. 6 to a fourth 2-3-2-4 compound with T_c estimated at 150 K). In addition, these newer Bi and Tl HTS materials lack a feature present in the yttrium 1-2-3 compound that was previously thought to be essential to superconductivity in these oxides; linear copper-oxygen chains (not illustrated in Figs. 4 or 5). Even the presence of copper-oxygen planes does not appear to be a prerequisite for superconductivity, as a new non-copper-containing oxide (a perovskite in the Ba-K-Bi-O system) with a T_c near 30 K has also recently been discovered (Ref. 16). A recent paper (W.A. Goddard at an American Chemical Society meeting on September 26, 1988) predicted that any copper oxide type of superconductor is limited to a maximum T_c of about 225 K, although also stating that the replacement of oxygen by other anions might raise this temperature.

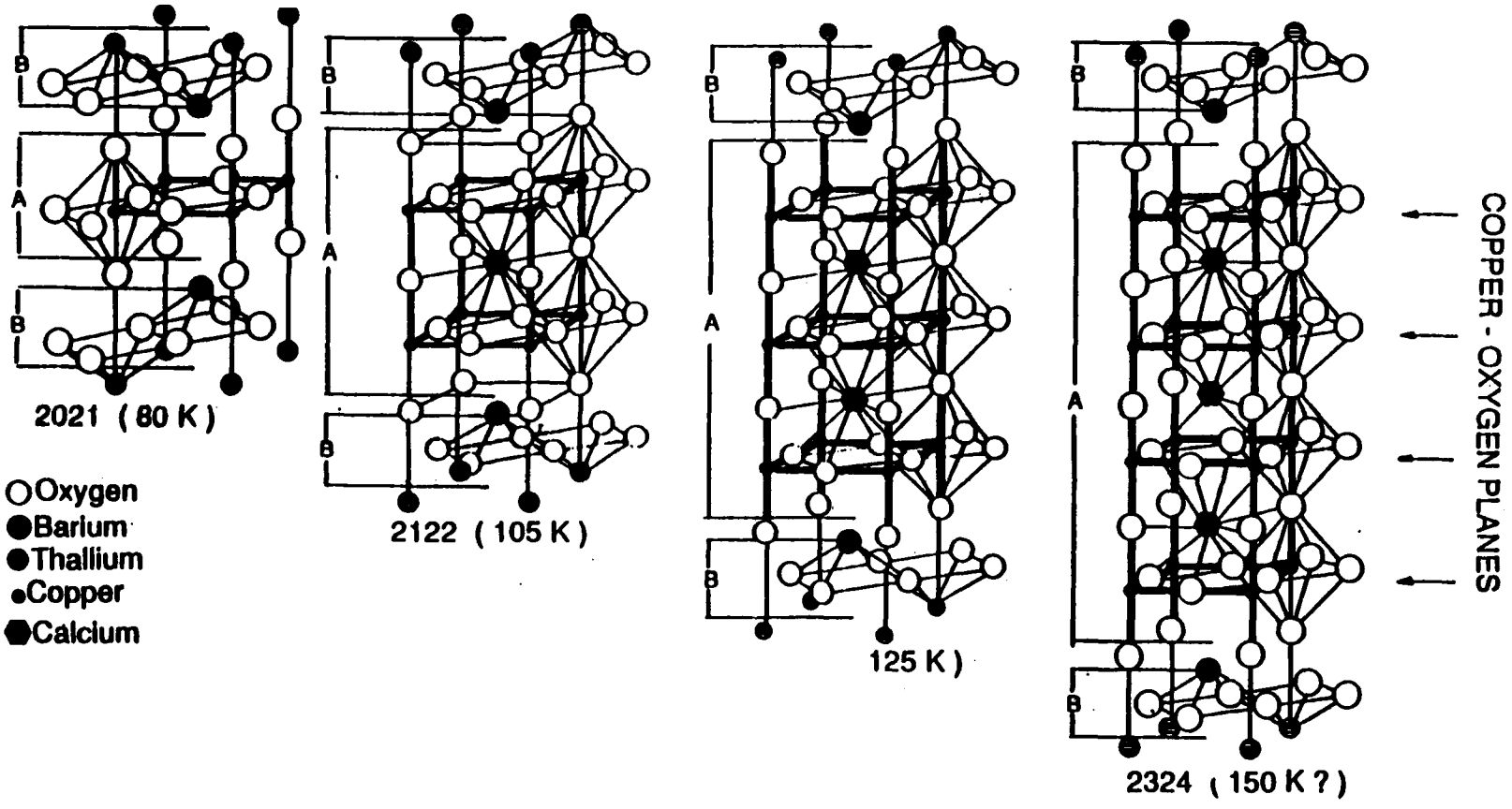

Figure 6. Crystal Structures of the Three Known Thallium-Containing Superconductors, Illustrating the Increasing Numbers of Adjacent Copper-Oxygen Planes Coincident with Higher T_c. The numbers designating each compound are the ratios of thallium, calcium, barium, and copper, respectively, in their chemical formulas; the last structure on the right is for a presumed material with even higher T_c.

These findings in connection with the discovery of new, higher T_c materials appear to confirm the assessment that the mechanism for superconductivity in oxides has not been determined. It seems clear that future research directed toward the structural causes of high T_c superconductivity may require looking beyond the mechanisms which physicists have proposed so far (Ref. 17).

IV. BOLOMETRIC INFRARED DETECTORS

A. BACKGROUND DISCUSSION

Bolometers are widely used broadband infrared detectors for slowly varying signals at far infrared wavelengths. The bolometric effect involves a change in the electrical resistance of a material due to temperature changes caused by absorbed radiation. As is well known (see, for example, Ref. 18), the increase in the bolometer's temperature is governed by the following differential equation

$$C\frac{d\Delta T}{dt} + K\Delta T = \frac{dP}{dT}\Delta T + \varepsilon\Delta\phi \quad , \tag{1}$$

where

C is the heat capacity of the material (JK^{-1})

K is the thermal conductance between the element and a heat reservoir (WK^{-1})

P is the thermal power generated by $I^2 R_d$ heating (W)

$\Delta\phi$ is an incremental increase in the power of the incident radiation (W)

ε is the detector emissivity (-) .

The rate of change of Joule heating with temperature. dP/dT, depends upon the details of the biasing circuit. However, by assuming an effective thermal conductance given by

$$K_e = K - \frac{dP}{dT} \quad ,$$

equation (1) can be written as

$$C\frac{d\Delta T}{dt} + K_e\,\Delta T = \varepsilon\Delta\phi \quad . \tag{2}$$

For a sinusoidally varying radiation field

$$\Delta\phi = \Delta\phi_0 e^{i\omega t} \quad .$$

The solution of equation (2) is

$$\Delta T = \Delta T_0 \exp\left(-\frac{t}{\tau}\right) + \frac{\varepsilon \Delta \phi}{K_e (1 + i\omega\tau)} \quad , \tag{3}$$

where τ (= C/K_e) is the thermal time constant of the device. For typical bolometers, τ lies in the range of milliseconds to seconds. Since the first term in equation (3) represents a transient which (under normal operating conditions) can be neglected with no loss of generality, the change in temperature of the bolometer due to the incident radiation can be written as

$$\Delta T = \frac{\varepsilon \Delta \phi_0}{K_e (1 + \omega^2\tau^2)^{1/2}} \quad . \tag{4}$$

From equation (4) it follows that in order to maximize ΔT, K_e must be small and $\omega\tau << 1$. Thus, the detector's thermal coupling to its surroundings as well as its heat capacity should be as small as possible.

Having determined the increase in temperature produced by the incident radiation, it is necessary to calculate the resulting change in the bolometer's resistance. This in turn determines the detector's output and so its responsivity. The fractional change in resistance due to a change in temperature is given by

$$\frac{\Delta R_d}{R_d} = \frac{1}{R_d} \frac{dR}{dT} \Delta T = \alpha \Delta T \quad , \tag{5}$$

where α is the temperature coefficient of resistance. For a simple biasing configuration (Fig. 7), the output signal is

$$\Delta V = \frac{R_L}{(R_d + R_L)^2} V_B \Delta R_d \quad , \tag{6}$$

where R_L is the load resistance and V_B is the bias voltage. Since the detector's responsivity is defined as

$$R = \frac{\Delta V}{\Delta \phi_0} \quad ,$$

it follows from equations (4)-(6) that

$$R = \left(\frac{R_L}{R_L + R_d}\right) \frac{I_B \varepsilon \alpha R_d}{K_e (1 + \omega^2\tau^2)^{1/2}} \quad , \tag{7}$$

where I_B is the bias current. From this equation it can be seen that in addition to minimizing K_e and C, it is desirable to maximize R_d, I_B, and α. Unfortunately, these cannot be varied independently. For example, since R_d must be matched to the input

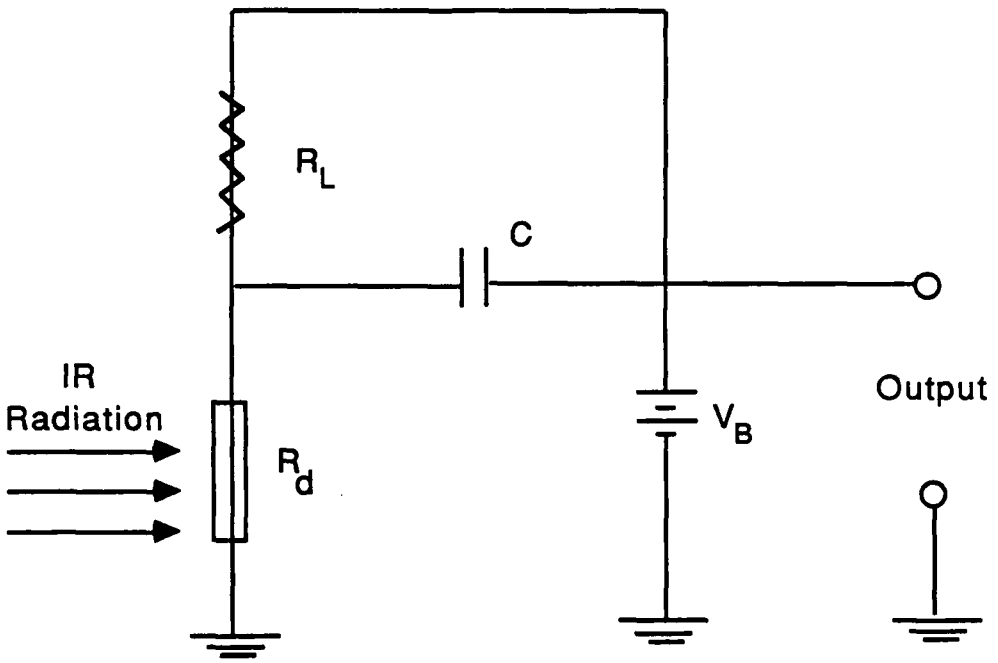

Figure 7. A Simple Biasing Configuration for a Bolometer.

impedance of the amplifier, its value is somewhat limited. Moreover, as R_d increases, both the Johnson noise and the RC time constant (due to the stray capacitance of the connecting leads) of the device will increase. Likewise, increasing the bias current increases the detector's 1/f noise. Finally, the temperature coefficient of resistance is, to a large extent, determined by the choice of detector material. Thus, although R_d, I_B, and α must be optimized, minimizing K_e and C provides the most direct way to improve device performance.

In order to determine the detector's sensitivity, it is necessary to consider the various noise sources that affect its performance. These can be divided into three categories: background (or radiation) noise, noise within the detector itself, and noise associated with the electronics following the detector. Begin by considering the background noise.

If the incident background radiation has a mean square fluctuation $\overline{\Delta W^2}$, this will cause a corresponding voltage fluctuation given by

$$\overline{V_{BN}^2} = R^2 \, \overline{\Delta W^2} \quad . \tag{8}$$

It can be shown that

$$\overline{\Delta W^2} = \frac{4\pi(k_B T_B)^5}{c^2 h^3} \, \alpha \cos(\theta) \, A_d \Delta f \int_0^\infty \frac{x^4 e^x}{(e^x - 1)} \, dx$$

(Ref. 19), where

T_B is the temperature of the background (K)

α is the solid angle subtended by an element of background at the detector (sr)

θ is the angle between the direction of sight and the normal to the detector (rad)

A_d is the area of the detector (cm^2)

Δf is the electrical bandwidth of the system (Hz)

$x = h\nu/k_B T_B$.

The amount of background radiation present is determined by both the angular acceptance of the optical system and the bandpass of any filters used. The noise voltage as a function of background temperature for a 0.2 sr angular acceptance is shown in Fig. 8. Figure 9 shows the noise voltage as a function of the angular acceptance for a background temperature of 300 K. Since the background temperature is fixed by the scenario in which the detector must operate, the only means left to the designer for controlling the level of background noise is the angular acceptance of the optical system. These decisions must be made on the basis of system level considerations.

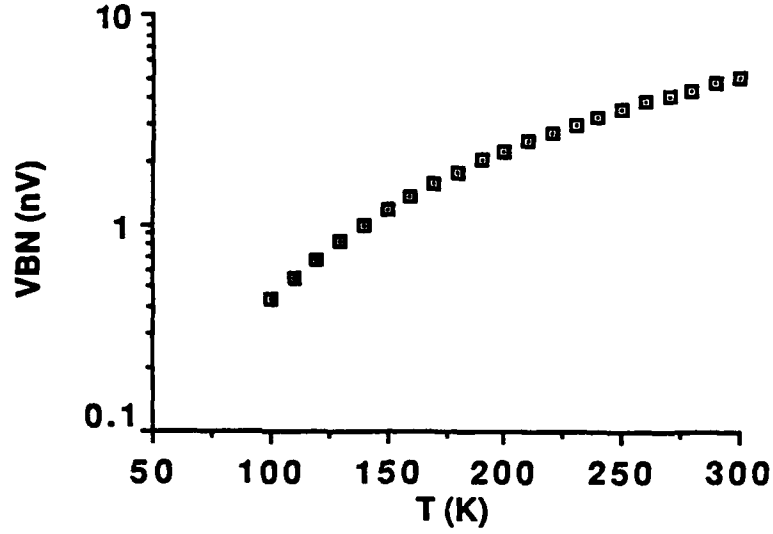

Figure 8. Background Noise Voltage as a Function of Background Temperature.

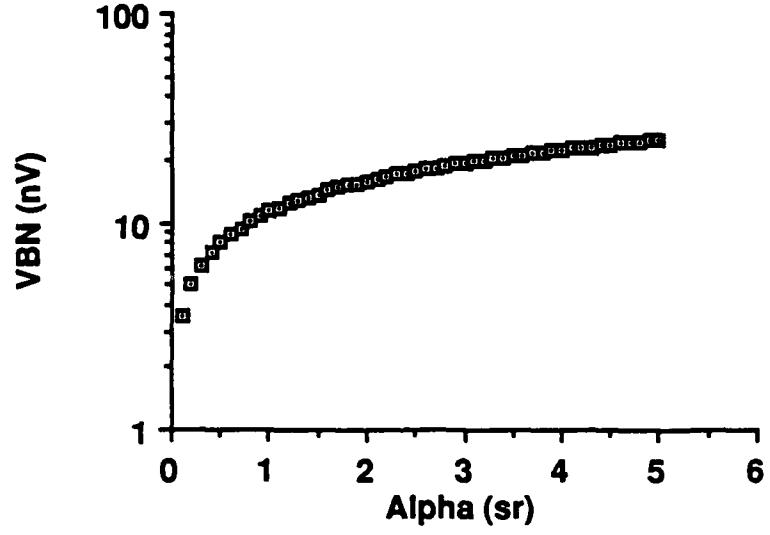

Figure 9. Background Noise Voltage as a Function of Angular Acceptance for a Fixed Background Temperature T_B = 300 K.

The detector noise involves three components: Johnson noise, thermal noise, and 1/f noise. Johnson noise results from the random motion of charge carriers in a resistive element. The noise voltage is given by

$$\overline{V_{JN}^2} = 4k_B T_d R_d \quad , \tag{9}$$

where T_d is the temperature of the detector and R_d is its resistance. Thermal noise results from fluctuations in the temperature of the device, caused by either radiative or conductive exchange with the surroundings. These fluctuations produce fluctuations in the signal voltage given by

$$\overline{V_{TN}^2} = 4k_B T_d^2 K \quad , \tag{10}$$

where K is the thermal conductance. The Johnson and thermal noise are plotted as a function of temperature in Fig. 10. Typical operating parameters for semiconductor bolometer have been used for these calculations, and are listed in Table 1. As can be seen in Fig. 10, while Johnson noise dominates at low temperatures, as the temperature is increased the detector's performance is eventually determined by thermal noise in the device. From equations (9) and (10) it can be seen that the temperature at which thermal noise dominates is proportional to the detector's resistance (R_d). So as R_d goes to zero (as

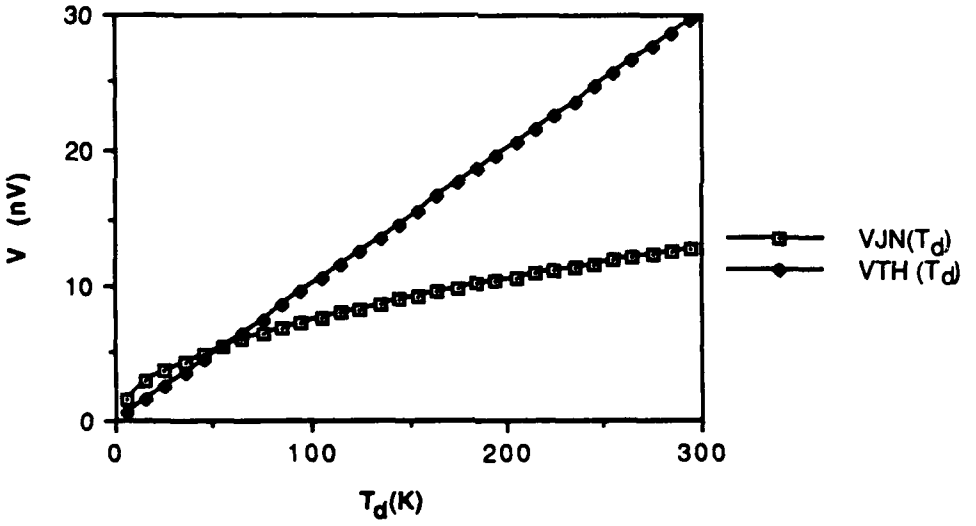

Figure 10. Johnson and Thermal Noise as a Function of Detector Temperature

Table 1. Typical Operating Parameters for a Semiconductor Bolometer

Area of Detector (A_d)	0.15 cm^2
Detector Resistance (R_d)	10^4 ohms
Responsivity (R)	10^3 V/W
Electrical Bandwidth (Df)	1 Hz
Thermal Conductance (K)	1.83×10^{-4} W/K

would be the case for a superconducting bolometer), this temperature also goes to zero. Thus, the fundamental limit to the performance of a superconducting bolometer is given by the thermal noise in the device. The implications of this fact with regard to bolometers fabricated from HTS materials will be discussed below.

Both thermal and Johnson noise will occur in an ideal detector. In any real device there will be additional noise sources, the most important of which is known as 1/f noise. Although the mechanism for this noise source is not well understood, it is characterized by a 1/f power spectrum and is observed to increase with increasing bias voltage. Thus, this component of the total noise can play an important role in the performance of thermal detectors. However, it can be minimized by the proper design and choice of operating characteristics and will not be considered further here.

Finally, there is noise associated with the electronics which follows the detector. With the development of low-noise field effect transistor (FET) amplifiers, this noise source is not as significant as it was in the past, and so will be ignored in what follows.

Assuming that the noise sources are statistically independent, it is possible to write the total noise voltage as

$$\overline{V_N^2} = \sum_i \overline{V_i^2} \quad . \tag{11}$$

A useful figure of merit for infrared detectors is the Noise Equivalent Power (NEP), which is defined as that value of signal power required o produce a signal-to-noise ratio of unity. It can be shown that

$$NEP = \frac{V_n}{R} \quad , \tag{12}$$

where V_n is the noise voltage [given by equation (11)] and R is the detector's responsivity.

In low background conditions the detector is limited by either Johnson noise or thermal noise. In such cases, the ultimate sensitivity of the device can be significantly improved if it is cooled to a very low temperature (cf. Fig. 10). Moreover, as the operating temperature is lowered, the material's temperature coefficient of resistance increases and its specific heat decreases. These also contribute to a higher responsivity.

B. SUPERCONDUCTING BOLOMETERS

To capitalize on the above effects, some of the first cooled bolometers used superconducting elements. To date, three types of superconducting bolometers have been developed. The transition edge bolometer is operated at a temperature within the material's transition region. Due to the abruptness of the transition, the temperature coefficient of resistance is quite large, and so the small temperature change produced by the absorbed radiation causes a dramatic change in the resistance of the detector. It is important to note that extremely good temperature control is required in order to maintain the device at the transition temperature. In addition to this device, two other types of superconducting bolometers have been built. The semiconductor-normal metal superconductor (SNS) bolometer uses the temperature dependence of the Josephson current in an SNS junction. Related to this is a third device, known as the superconductor insulator normal (SIN) bolometer, which utilizes the temperature dependence of the quasi-particle current through a superconductor-insulator-normal metal junction. Except for the junctions involved, the construction of the SNS and SIN devices is similar to that shown in Fig. 11 for the transition-edge bolometer. This device consists of a thin film deposited onto a sapphire substrate, which is covered on the opposite side with a thin bismuth film to absorb the incident radiation. These so-called composite bolometers were designed to achieve smaller thermal conductances (thereby improving device sensitivity), while maintaining reasonable thermal time constants.

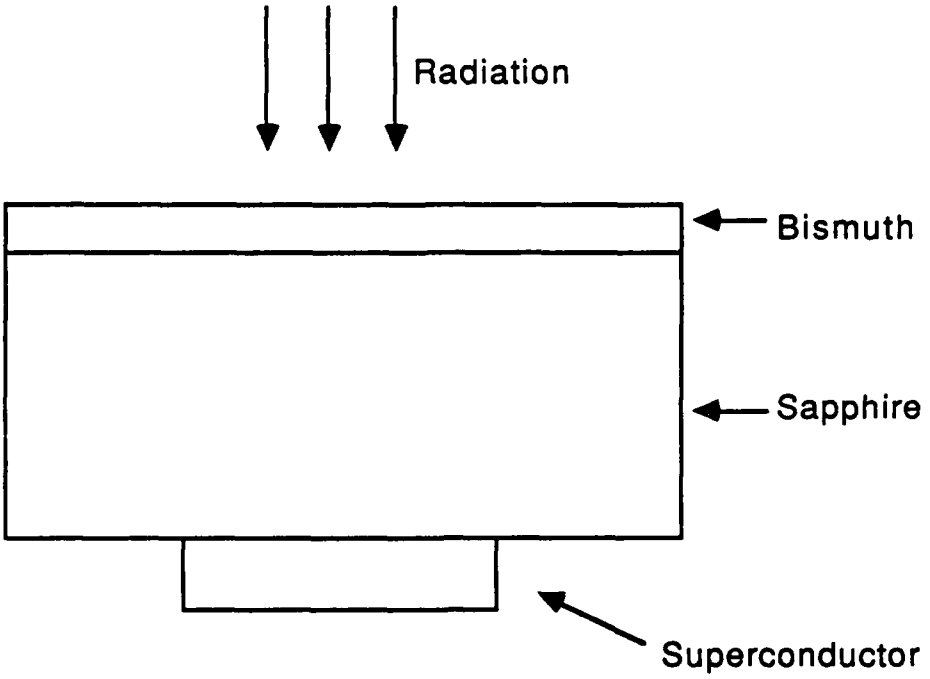

Figure 11. A Composite Bolometer

Table 2 shows the performance that has been achieved to date with the various types of bolometers. As mentioned above, the theoretical limit of the NEP is determined by the thermal noise in the device, i.e.,

$$(NEP)_{th} = \sqrt{4k_B T^2 K} \quad . \tag{13}$$

Note that the measured values of NEP are given in terms of the electrical (as opposed to optical) power dissipated. Due to the poor coupling between the detector and the radiation field, the optical NEP is roughly a factor of two higher than the electrical NEP. For comparison, a low-temperature, gallium-doped germanium bolometer is also included. As can be seen, the transition edge and SNS devices have sensitivities comparable to the semiconductor bolometer. In fact, both superconducting and non-superconducting detectors have nearly ideal NEPs. From equation (13) it follows that further advances depend on building devices with small thermal conductances. However, in order to maintain a reasonable frequency response, such improvements must be accompanied by

Table 2. Various Bolometer Characteristics

Bolometer Type	Theoretical NEP (W)	Observed NEP (W)*	Time Constant (s)	Temperature (K)
Al Transition Edge[20]	1.3×10^{-15}	1.7×10^{-15}	0.08	1.3
Pb/CuAl/Pb SNS[21]	1.1×10^{-15}	5.0×10^{-15}	3.0	1.5
$Pb/Al_2O_3/Al$ SIN[21]	1.1×10^{-15}	1.0×10^{-15}	--	1.5
Ge:Ga[22]	2.2×10^{-15}	3.0×10^{-15}	0.003	1.2

* The observed sensitivities are given in terms of electrical NEPs (cf. text).

lower heat capacities. Some possibilities along these lines include replacing the bismuth absorber with a thinner chromium film and the sapphire substrate with diamond (diamond has a specific heat roughly a factor of 10 less than that of sapphire). At some point, however, the heat capacity of the film will dominate, and so limit these improvements.

It has recently been suggested that bolometers be fabricated from high-temperature superconducting materials. It is important to realize, however, that certain trade-offs are implicit in such a decision. On the one hand, the ultimate sensitivity of such a device would be less than that of more conventional bolometers. This is due to two effects. First, the heat capacity of these materials is somewhat larger than that of conventional superconductors. At the point where the heat capacity of the film limits the device performance, it follows that using high temperature superconductors would in fact lessen the ultimate sensitivity. A more important consideration, however, concerns the temperatures at which devices based on these new materials would operate. As discussed above, the fundamental limit to the performance of a superconducting bolometer is given by the thermal noise in the device (i.e., NEP ~ $K^{1/2}T$). Thus, the higher operating temperatures involved would degrade the performance. For example, if all else is equal, the ultimate sensitivity of a bolometer operated at 80 K is NEP ~ 10^{-14} W. This is an order of magnitude worse than a device operated at 5 K. On the other hand, for satellite applications in which size, weight, and reliability of the detector's cryogenic equipment is crucial, bolometers based on high-temperature superconducting materials give the system designer an additional degree of freedom. For some applications, this consideration may outweigh the poorer performance. It must be pointed out in this context that there are

numerous efforts underway to develop room-temperature bolometric devices for certain high-volume applications requiring only moderate performance.

C. CONCLUSIONS

Although low-temperature superconducting materials can be used to fabricate extremely sensitive bolometers for low background conditions, the situation does not look as promising for bolometers made from high-temperature superconductors. The problem in the latter case involves poor performance resulting from increased thermal noise. Although it is possible that system level considerations (such as the weight and power required by the cryogenic system) could outweigh the lower performance, the consensus seems to be that bolometers fabricated from high-temperature superconductors do not hold much promise. It should be noted in this context that there are numerous efforts underway to develop uncooled (i.e., room temperature) bolometric devices. It would be interesting to compare the performance of these detectors with bolometers based on high-temperature superconductors.

V. DIRECT SUPERCONDUCTOR INFRARED DETECTORS

A. BACKGROUND DISCUSSION

In addition to infrared bolometers, recent efforts have focused on Josephson Junctions as direct IR detectors. The detection mechanism in this case is based on the non-equilibrium state of the superconductor caused by the incident radiation. When optical flux is absorbed by the material, Cooper pairs are broken, thereby exciting excess quasi-particles. These quasi-particles will depress the superconducting energy gap. This can be seen by the following argument. Consider an electron with momentum **p** and spin up ($\mathbf{p}\uparrow$). Without a corresponding electron in the state ($-\mathbf{p}\downarrow$) the pair state ($\mathbf{p}\uparrow$, $-\mathbf{p}\downarrow$) cannot be occupied. The electron-electron interaction energy is then smaller since the number of scattering events in which the electrons can participate is smaller. According to the BCS theory, the superconducting energy gap is given by (Ref. 23)

$$\Delta = 2h\upsilon_L \left[\exp\left(1/\rho(E_f)M\right) - 1\right]^{-1} ,$$

where υ_L is the average phonon frequency, M is the matrix element of the scattering interaction and $\rho(E_f)$ is the density of states for electrons at the Fermi energy. Thus, the decrease in the pair interaction energy (M) causes a decrease in the superconducting energy gap.

The Josephson current across the junction can be written as a function of the energy gap as follows (Ref. 24)

$$I_c = \pi\left[\frac{\Delta(T)}{2eR_n}\right] \tanh\left[\frac{\Delta(T)}{2k_BT}\right] , \qquad (14)$$

where

$\Delta(T)$ is the energy gap (J)

e is the charge on the electron (Coulomb)

R_n is the normal state resistance of the junction (Ohm)

T is the temperature of the junction (K).

Assuming that this equation holds in the non-equilibrium state, it can be seen that decreasing the superconducting gap will in turn change the I-V characteristics of the junction. Thus, when such a device is current biased, its voltage is sensitive to infrared radiation.

It has recently been suggested (Ref. 25) that IR detection in Josephson Junction devices is due to a thermal mechanism. This idea deserves a brief mention. The original work in this area was done in 1971 by L.R. Testardi (Ref. 26). By studying the dc resistance of superconducting Pb films subjected to pulsed laser light, he concluded that for $T < T_c$ the observed superconducting-to-normal transition induced by the radiation could not be accounted for by sample heating. Instead, he suggested that excess (i.e., non-equilibrium) quasi-particles created by photon pair-breaking were responsible. For $T \geq T_c$, on the other hand, Testardi found that thermal effects do in fact dominate the material's optical response. Following this, C.S. Owen and D.J. Scalapino calculated the energy gap of a BCS superconductor in which an excess quasi-particle density is maintained by a radiation field (Ref. 27). It was assumed that the quasi-particles are in equilibrium among themselves in a Fermi-Dirac distribution characterized by some chemical potential (which is not equal to that of the Cooper pairs) and a temperature equal to the lattice temperature. They showed that for $T < T_c$, the energy gap as a function of the excess quasi-particle density can be written as

$$\frac{\Delta}{\Delta_0} = 1 - 2n \quad ,$$

where Δ is the energy gap of the material in its non-equilibrium state, Δ_0 is the energy gap at zero temperature, and n is the excess quasi-particle number in units of $4\rho(Ef)\Delta_0$, i.e.,

$$n = \frac{N - N_T}{4\,\rho(E_f)\,\Delta_0} \quad ,$$

where

N is the total quasi-particle density (cm^{-3})

N_T is the thermal equilibrium quasi-particle density (cm^{-3})

$\rho(E_f)$ is the electronic density of states at the Fermi level ($cm^{-3}\,eV^{-1}$).

This model was confirmed in 1972 by Parker and Williams (Ref. 28). These experiments, which involved laser illuminated tunnel junctions, found both a decrease in the energy gap

and an increase in the quasi-particle chemical potential upon illumination. Since this original work, further research has also confirmed these results. Thus, one must conclude that for devices operated at temperatures below the critical temperature, the optical response is due to the creation of excess quasi-particles and not to a thermal mechanism.

B. EXPERIMENTAL RESULTS (Low-Temperature Superconductors)

In the past few years numerous research groups have actually built detectors which operate according to this mechanism. Researchers at the Naval Research Laboratory (Ref. 29) prepared thin superconducting, granular films of NbN/BN for use as photodetectors for far infrared radiation ($\lambda > 100$ μm). The grain boundaries in this material behave like weak-link junctions and so these films can be thought of as random network of Josephson Junctions. The detectors, which operate at temperatures less than 7 K, have a spectral bandwidth of 50 μm to 500 μm. The observed sensitivity of the film decreases with decreasing wavelengths. In fact, at visible wavelengths, the responsivity of the device was roughly two orders of magnitude lower than it was for infrared radiation. This is due to the fact that the optical absorption in the superconducting film decreases with decreasing wavelengths. In addition to this broad bandwidth, the devices were relatively fast, having response times less than 1 ns. The sensitivity of the film was measured with a pulsed laser operating at a wavelength of 385 μm and a power level of 1 W. The responsivity was estimated to be about 0.2 V/W. The NRL group claimed that since the thickness of the film used in these experiments was only 7 nm, it may be possible to increase the responsivity by increasing the film thickness, thereby increasing the absolute absorption in the material. The rms noise voltage was measured (with only ambient radiation present and the device current biased) with a lock-in amplifier and was found to be indistinguishable from the noise voltage of the measurement system. This gave an upper bound on the noise level of 0.1 μV. Based on these measurements, a noise equivalent power of approximately 5×10^{-7} W was reported. Unfortunately, the NRL measurement of the detector noise was too crude to be useful in predicting the ultimate performance of their device.

Workers at NTT's Electrical Communications Laboratory in Japan recently reported using a perovskite-type thin film superconductor, $BaPb_{1-x}\ Bi_x\ O_3$, as an optical detector (Ref. 30). As in the NbN/BN case, the grain boundaries in the material behave as weak-link devices, and so are responsible for the direct detection of the IR radiation. The Japanese began this work by studying the optical properties of the material. In particular

they measured the reflectivity and absorption coefficient for wavelengths between roughly 1 and 20 μm. The dominant feature of this data is the plasma frequency, which occurs at 0.8 μm (BaPbBiO has a carrier concentration of ~ 10^{21} cm^{-3}, which is roughly two orders of magnitude less than most metals). For $\lambda > 0.8$ μm, the material exhibits a high absorption coefficient (~ 10^5 cm^{-1}) and a low reflection coefficient (~ 60 percent) over a large spectral band. However, if one assumes that the optical properties obey a Drude-like theory, (in which the absorption coefficient goes as $1/\omega^2$ for frequencies greater than or equal to the plasma frequency) a $\lambda = 0.8$ μm plasma edge suggests lower absorption for visible light and hence fairly low performance in this part of the spectrum. The BaPbBi0 device was operated at a temperature of 6 K. Although the experiment was restricted to wavelengths from 1 μm to 8 μm, the 1 meV energy gap of this material suggests that the spectral bandwidth could be extended past 500 μm. The responsivity of this detector, which was measured with a diode laser operating at 1.3 μm, was reported as 10^4 V/W. A detectivity of $D^* \sim 3.0 \times 10^{10}$ cm $Hz^{1/2}/W$ was estimated on the basis of a theoretical speculation concerning the noise in the device. Because the noise in these devices is not well understood, this value is highly suspect. Finally, the frequency response for the BaPbBiO device was quite high, with response times less than 1 ns.

Note that care must be taken when comparing these numbers to the NRL results. Not only was the film thickness roughly a factor of 20 different, but (more importantly) the two measurements were done in different spectral regions: the NRL results were obtained for $\lambda \sim 500$ μm whereas the Japanese work was performed at $\lambda \sim 5$ μm. Needless to say, the optical properties (in particular the absorption coefficients) vary widely over such a range. Whether or not such differences can account for the size of this discrepancy is still an open question.

C. EXPERIMENTAL RESULTS (High-Temperature Superconductors)

The Japanese results are very encouraging in light of the discovery of high temperature superconductivity in the compounds $La_{2-x}Ba_xCu0_4$ and $YBa_2Cu_30_{7-x}$. Like BaPbPBiO, these materials have a low electron concentration, low reflectivity, and a high absorption coefficient in the infrared and hence may also be sensitive IR detectors. Numerous groups are trying to develop IR detectors based on high-temperature superconducting materials. They include the following organizations:

Naval Research Laboratory
Los Alamos National Laboratory
Sandia National Laboratory
National Bureau of Standards (Boulder)
Stanford University
Cornell University
University of Alabama
Westinghouse Corporation
Hypress Corporation
TRW Corporation
Honeywell Corporation
Hughes Aircraft Company.

Some of these efforts are briefly summarized below.

Dr. M. Leung and collaborators at the Naval Research Laboratory recently reported using a thin granular film of $YB_2Cu_3O_{7-x}$ as an optical detector (Ref. 31). The film had a transition temperature of 35 K, with an onset temperature of 80 K. They measured the temperature dependence of the detector's response and found that the curve had a maximum near 30 K. This is thought to result from the temperature dependence of the Josephson coupling between grains in the material. This effect is interesting in light of the discussion (referred to above) concerning the possibility that the optical response of these films is dominated by a thermal mechanism. Since a bolometric response is proportional to the material's temperature coefficient of resistance (dR/dT) (cf. equation 7), one would expect the detector's response to peak in the middle of the transition region, which in this case is roughly 60 K (cf. Fig. 1 of Ref. 31). Instead, the response drops from a maximum value of 70 μV at 30 K to 20 μV at 60 K. This provides further evidence that the detection mechanism in Josephson Junction IR detectors (operated at temperatures below the transition temperature) is not thermal in origin. A blackbody source at 900 K was used to measure the detector's responsivity and noise equivalent power. Unfortunately, they used quartz windows on the Dewar which turn-off from 3 μm to 60 μm (Ref. 32). Thus, when determining the total optical power incident on the device they had to convolve the quartz transmission spectrum with that of the blackbody source. How carefully this was done and what effect it may have had on the measurements was not stated. This notwithstanding, they reported detectivity of $D^* \sim 10^6$ cm $Hz^{1/2}/W$. This poor performance was due to the high noise voltage that was present in the device. Examination of the noise characteristics

showed that the noise voltage was proportional to the square root of the bias current, thereby indicating that the noise was in fact shot noise. Workers at NRL believe that this noise arose from non-ohmic electrical contacts to the device. Thus, as has been the case with all of the work reported to date on the performance of superconducting tunnel junction IR detectors, there is no clue concerning the intrinsic noise sources in these devices. Without such data it is impossible to assess the fundamental limits on the performance of these novel IR detectors.

The Air Force Office of Scientific Research (AFOSR) has recently begun funding work at Stanford University on superconducting IR detectors. Early in the first phase of this work they were able to control the orientation and microstructure of thin films of $YBa_2Cu_3O_{7-x}$, and found that the electrical and optical properties of the different films were quite diverse. Thus, it was decided to prepare numerous films, each with a well-characterized microstructure and then to compare their optical properties. Although this work is currently in progress, some results have been obtained. The optical properties of the so-called "123 compounds" seem to be very similar to those of BaPbBi0. In particular the reflection spectra can be explained by a simple Drude theory with a plasma edge at 2.6 eV (λ = 0.5 μm) (Ref. 33). Thus, in the spectral range 2 μm < λ < 10 μm the reflectivity falls slowly from 90 percent (at 10 μm) to 60 percent (at 2 μm). As one approaches the plasma edge, it begins to fall faster and then levels out to roughly 10 percent in the visible portion of the spectrum. While this sounds promising for potential applications in the visible, it should be remembered that if the absorption also behaves according to a Drude theory, it will fall off as $1/\omega^2$ in the visible. Thus, the device performance in this part of the spectrum may be considerably worse.

It should be noted that large sample-to-sample variations in the optical properties of these materials were observed, despite the fact that the films showed very similar transport properties. There appear to be two main reasons for this variation. First, the as-grown films often have non-superconducting phases on their surfaces. By removing this impurity phase, a high reflectance can be obtained. The second source of variability involves the different orientations of the various grains present in the films. This anisotropy in the optical properties is particularly severe for mid-IR radiation--it decreases as the photon energy is increased and essentially disappears for λ < 6000 Å.

The Stanford group has also determined that the optical penetration depth for mid-IR radiation is around 1000 Å. For lower frequencies, this depth decreases due to free carrier absorption. This suggests that for optimum device performance one should use

films whose thickness is 1000 Å or less. This is in contrast to previous work which suggested 1 to 10 μm as the optimum thickness.

Another effort funded by AFOSR is being carried out by Westinghouse. This work will be divided into three phases and will stretch over the next two years. In the initial phase Westinghouse hopes to develop both a patterning process for high-temperature superconducting thin films and low-resistance, low-noise contacts for these materials. They will also start measuring the optical response of currently available thin films. At present, 90 percent of this initial phase has been completed. In particular, pattern linewidths of 5 μm are now routine and (more importantly) the patterning process does not degrade the superconducting properties of the thin films. Unfortunately, the optical response of the devices is somewhat disappointing in that only a bolometric response has been observed. Westinghouse attributes this to the absence of any weak-link structure in the films. Preliminary measurements at $\lambda = 0.6$ μm gave a responsivity of 2000 V/W and a detectivity of 10^7 cm $Hz^{1/2}$ W^{-1}. Because these results are preliminary, Westinghouse is unable to account for the high noise levels that are dominating device performance. They are, however, currently refining their noise measurement capabilities.

The second phase of the Westinghouse effort involves investigating the correlations between the film's granularity and its optical and superconducting properties. In particular they hope to be able to "dope" the grain boundaries in the material in order to control the nature of the intergrain (i.e., Josephson) coupling. This research is currently in progress and no results have been reported. The final phase of this work will involve comparing the performance of IR detectors based on high-temperature superconducting materials with semiconductor devices.

Los Alamos National Laboratory (LANL) has recently received a grant from SDIO to study IR detectors based upon high-temperature superconducting materials. This work will include various materials systems and will involve thin film materials development as well as detector characterization. To date, LANL has made a 3×3 test array in order to determine how to make low noise contacts to these materials. Although no performance data has yet been taken with this device, they were able to make low noise contacts to the test array. This result, coupled with that from Westinghouse, suggests that making contact to this material may not be as difficult as originally thought. In order to do further testing low noise pre-amps will be required. For this aspect of the work LANL will be teaming with Aerospace Corporation. With a low noise front-end they will be able to investigate the intrinsic sources of noise in these devices. The importance of such measurements cannot

be overestimated--without an understanding of the intrinsic noise in these devices it is impossible to determine the fundamental limits on the performance of superconducting IR detectors.

D. CONCLUSIONS

The situation for direct superconductor IR detectors is not clear. As is well known, the ultimate performance of *any* IR detector occurs when the noise generated by the fluctuations in the background flux incident on the device is larger than the thermally generated noise within the detector itself. This suggests that the detector noise, *not* its responsivity, drives device performance. The responsivity is important only in that it must be large enough to ensure that the sensor is not system noise limited. This fact seems to have escaped many investigators currently working in this field. As a result, the only measurements reported to date involve the detector's responsivity, with only lip service being given to noise measurements. In the case of HTS IR detectors this lack of data is especially troublesome. Recall that these devices are being sold on the premise that they will allow higher temperature operation. But the operating temperature for any IR detector is determined by the amount of thermal noise that can be tolerated for a given application. To date, there has been no satisfactory work reported in this area. Until this question is resolved, other efforts in this field seem premature. With this in mind, IDA has recently begun to consider the thermal noise in superconducting IR detectors. While the results are interesting, they are very preliminary and will be reported later.

VI. A NOTE ON SUPERCONDUCTING ELECTRONICS

It has been remarked that one of the most important applications of high temperature superconductivity in infrared detection may be in the area of signal processing. A typical focal plane array requires the following "backplane electronics":

Photocurrent integration

Charge-to-voltage conversion

Multiplexing

A/D conversion

Gain and offset corrections

Background subtraction and clutter suppression

Filtering, track formation, etc.

The first three items are, in general, located on the focal plane and so are operated at cryogenic temperatures. In order to achieve a total power dissipation of less than 1 W, it is necessary that each channel of the device dissipate something less than 10 μW. Given their high speed and low power dissipation, superconducting electronics would be ideally suited for such applications. Moreover, since the A/D converters in these systems consume far too much power to be located on the focal plane, the analog signals must be brought out of the dewar to the remaining electronics. The capacitance of these leads can invite a variety of problems. If the A/D converter could be fabricated with superconducting materials, it could be moved onto the focal plane, thereby greatly simplifying the sensor. It is important to note that this would be an important contribution to any IR system, regardless of the type of detector. Unfortunately, fabricating low-noise Josephson Junction devices is difficult, even with conventional superconductors. Thus, such applications will be realized in high-temperature superconductors only in the long term. One interesting possibility along these lines might be to use a semiconductor detector (such as extrinsic silicon), and low-temperature superconducting materials for the signal processing. This combination would be achievable in a much more realistic time frame.

VII. REFERENCES

1. B. Balko, L. Cohen, R. Collins, J. Hove, and J. Nicoll, "Central Research Project Report on Superconductivity (FY 1987)," IDA Memorandum Report M-468, May 1988.

2. J.G. Bednorz and K.A. Muller, "Possible High T_c Superconductivity in the Ba-La-Cu-O System," *Zeit. Phys. B*, **64**, 189-93, 1986.

3. M.K. Wu, J.R. Ashburn, C.J. Torng, P.H. Hor, R.L. Merg, L. Gao, Z.J. Huang, Q. Wang, and C.W. Chu, "Superconductivity at 93 K in a Mixed-Phase Y-Ba-Cu-O Compound System at Ambient Pressure," *Phys. Rev. Lett.*, **58**, 908-910, 1987.

4. D.Klibanow, K. Sujata, and T.O. Mason, "Solid Phase Relations at 950 °C in La-Ba-Cu-O," *J. Am. Ceram. Soc.*, **71**, C-267 - C-269, 1988.

5. Robert M. Hazen, "Perovskites," *Sci. Am.*, 74-81, June 1988.

6. G. Wang, S.J. Hwu, S.N. Song, J.B. Ketterson, L.D. Marks, K.R. Poeppelmeier, and T.O. Mason, "950 °C Subsolidus Phase Diagram for Y_2O_3-BaO-CuO System in Air," in *Adv. Ceram. Mater.*, **2** [3B, Special Issue], 313-326, 1987.

7. K.G. Frase and D.R. Clarke, "Phase Compatibilities in the System Y_2O_3-Ba-O-CuO," in Ref. 6, 295-302.

8. R.S. Roth, K.L. Davis and J.R. Dennis, "Phase Equilibria and Crystal Chemistry in the System Ba-Y-Cu-O", in Ref. 6, 303-312.

9. Ron Dagani, "New Class of Superconductors Pushing Temperatures Higher," *C&EN*, 24-29, 16 May 1988.

10. R.M. Hazen, et. al., "Superconductivity in the High-T_c Bi-Ca-Sr-Cu-O System: Phase Identification," *Phys. Rev. Lett.*, **60**, 1174-1177, 1988.

11. C. Michel, et.al., *Z. Phys. B*, **68**, 421, 1987.

12. C.W. Chu, et. al., "Superconductivity up to 114 K in the Bi-Al-Ca-Sr-Cu-O System without Rare Earth Elements," *Phys. Rev. Lett.*, **60**, 941-943, 1988.

13. R.M. Hazen, et. al., "100-K Superconducting Phases in the Tl-Ca-Ba-Cu-O System," *Phys. Rev. Lett.*, **60**, 1657-1660, 1988.

14. P. Ghosh, "Thallium puts Superconductivity on the Road to 200 K," *New Sci.*, 28, 7 April 1988.

15. D.R. Clarke, "The Development of High-T_c Ceramic Superconductors: An Introduction," in Ref. 6, 273-287.

16. R.J. Cava (AT&T Bell Laboratories), "Crystal Chemistry and Physical Properties of High T_c Superconductors," given at 90th Annual Meeting of the American Ceramic Society, Cincinnati, Ohio, 2 May 1988.

17. T. Cox, "Superconductivity Discovers the Chemical Bond," *New Sci.*, 64-66, 23 June 1988.

18. T. Limperis and J. Mudar, *The Infrared Handbook*, edited by G.J. Zissis and W.L. Wolfe, Office of Naval Research, Department of the Navy, Washington, DC, 1985.

19. E.H. Putley, *Infrared Phys.*, **4**, 1, 1964.

20. K. Rose, *IEEE Trans. Electron Devices*, **ED-27**, 119, 1980.

21. J. Clarke, G.I. Hoffer, P.L. Richards and N.-H. Yeh, *J. Appl. Phys.*, **48**, 12, 4865, 1977.

22. J. Clarke, G.I. Hoffer, and P.L. Richards, *Rev. Phys. Appl.*, **9**, 69 (1974).

23. C. Kittel, *Quantum Theory of Solids*, John Wiley & Sons, New York, 155, 1963.

24. V. Ambegaokar and A. Baratoff, *Phys. Rev. Lett.*, **10**, 486, 1963.

25. F. Quelle, *Small Device TIWG Meeting*; W.J. Schafer Co., Arlington, Va., May 24, 1988.

26 L.R. Testardi, *Phys. Rev.*, **B4**, 2189, 1971.

27. C.S. Owen and D.J. Scalapino, *Phys. Rev. Lett.*, **28**, 1559, 1972.

28. W.H. Parker and W.D. Williams, *Phys. Rev. Lett.*, **29**, 924, 1972.

29. M. Leung, U. Strom, J.C. Culberston, J.H. Claassen, S.A. Wolf and R.W. Simon, *Appl. Phys. Lett.*, **50**, 23, 1691, 1987.

30. Y. Enomoto and T. Murakami, *J. Appl. Phys.*, **59**, 11, 3807, 1986.

31. M. Leung, P.R. Broussard, J.H. Claassen, M. Osofsky, S.A. Wolf, and U. Strom, *Appl. Phys. Lett.*, **51**, 24, 2046, 1987.

32. W.L. Wolfe: *The Infrared Handbook*, ed. by G.J. Zissis and W.L. Wolfe, Office of Naval Research, Department of the Navy, Washington, D.C., 1985.

33. I. Bozovic, et.al., *Phys. Rev. Lett.*, **59**, 2219, 1987